IOSR Journal of Applied Physics (IOSR-JAP)
e-ISSN: 2278-4861.Volume 8, Issue 2 Ver. I (Mar. - Apr. 2016), PP 01-08
www.iosrjournals

Lattice Dynamical Study of Indium Phosphide (InP)

Suresh Chandra Pandey[1], Jay Prakash Dubey[1*], Kripa Shankar Upadhyaya[2]
[1]*Department of Physics, Mahatma Ghandhi Gramodaya Vishwavidyalaya, Chitrakoo, Satna M. P., India*
[1*,]*Department of Physics, Dr. K.N. Modi University, Newai, Rajasthan, India*
[2]*Department of Physics, Nehru Gram Bharati University, Allahabad, U. P., India*

Abstract: *The complete lattice dynamics (phonon dispersion curves, Debye temperatures variation, combined density of states (CDS) curves, two-phonon Raman and anharmonic elastic properties) of InP with zinc-blende structure has been investigated by van der Waal's three body force shell model (VTSM). This model incorporates the effect of van der Waal's interactions and three-body interactions into the rigid shell model of zinc blende structure, where the short range interactions are operative upto the second neighbours. Our results are in good agreement with the available measured data. It is concluded that this model VTSM will be equally applicable to study above properties of other zinc-blende structure solids as compared to the models of earlier workers.*

Keywords: *Phonons , van der Waal's interactions , Debye temperatures variation , Combined density of states curve , Raman spectra , Phonon dispersion curves , Lattice dynamics , InP.*
PACS No: 63.20.-e, 65.40.Ba, 78.30.-j

I. Introduction

In recent years, there has been considerable interest in the theoretical and experimental studies of inelastic neutron scattering, a huge amount of experimental data has been accumulated for phonon dispersion curves of various II-VI and III-V compounds [1-5], crystallizing into the zinc-blende structure (ZBS). This particular attention is primarily due to their high symmetry and simplicity of their ionic bonding. These semiconductor crystals (InP, InAs and InSb) have remarkable property of transverse acoustic (TA) vibrations. The phenomenological models which have been used to calculate the frequencies of ZBS crystals can be broadly classified into two categories. (i) Rigid Ion Model (RIM) [6-8] and (ii) Shell Model [9-10]. The Valence Force Field Model (VFFM) as used by Price et al. [11] incorporates bond-bending, bond stretching and point Coulombic interactions [12]. Later on, the original 14-parameter VFFM was modified on the lines of shell model by Vageletos et al. [5] and Feldkamp et al. [13]. In addition to RIM, SNIM (Second Neighbour Ionic Model) and VFFM, some other models e.g., the bond charge model (BCM) and deformable dipole model (DDM) have also been used for zinc-blende crystals [14-15] and so on.

In this communication, we are mainly concerned with the lattice dynamical study of Indium Phosphide InP. The experimental data on InP for phonon dispersion curves [3, 4], harmonic and anharmonic elastic constants [16], Debye temperatures variation [17] and Raman spectra [18] are available. These workers have tried to interpret the phonon dispersion curves (PDCs) but none has succeeded in describing the PDCs and other results of InP very well. They have compared their theoretical results with their measured data but with only partial success.

Furthermore, effect of long range (LR) three body interactions (TBI), short range (SR) interactions and van der Waal's (VDW) attraction are significant, in partially ionic and covalent crystals [19]. Though, van der Waal's interactions have much effective force, but Singh and Singh [20] have used only three body force shell model (TSM) formulations for InP, InAs and InSb without inclusion of van der Waal's interactions (VDWI). So far, the calculations on third order elastic constants (TOEC) and pressure derivatives of second order elastic constants (SOEC) are concerned, Sharma and Verma [21] have reformulated the expressions derived by Garg et. al. [22]. They have derived the correct expressions for TOEC and pressure derivatives of SOEC for ZBS crystals. The various coresearchers (Upadhyaya et. al. [23, 24], Tiwari et. al. [25], Srivastava and Upadhyaya [26], Mishra and Upadhyaya [27], Dubey et. al. [28, 29]) used their correct expressions for calculating the anharmonic elastic properties for NaCl, CsCl and ZBS structure of solids. Therefore, we have used expressions of Sharma and Verma [21] as such for our computations.

The above informations have encouraged us to include (i) the effect of VDWI and (ii) TBI in the framework of RSM where short range interactions are effective upto the second neighbours. Our model thus developed is known as van der Waal's three body force shell model (VTSM). It has 14-parameters; four TBI parameters b, ρ, $f(r_0)$, $r_0 f'(r_0)$; six nearest and the next-nearest neighbour short-range repulsive interaction parameters (A_{12}, B_{12}, A_{11}, B_{11}, A_{22}, B_{22}), two distortion polarizabilities of negative and positive ions (d_1, d_2)and two shell charges of the negative and positive ions (Y_1, Y_2) respectively. They can be deduced with the help of

measured values of elastic constants, dielectric constants, electronic polarizabilities and van der Waal's coupling coefficients. This model has been applied to study the lattice dynamics of indium pnictides (InP, InAs, InSb). In this paper, we are reporting the study of phonon dispersion curves, Debye temperatures variation, combined density of states (CDS), third order elastic constants and pressure derivatives of SOEC of InP only. The formalism of our model has been presented in the next section in detail.

II. Theoretical framework of the present model

We have developed a model for ZBS structure, which includes the effect of van der Waal's interactions (VDWI) and three body interactions (TBI) in the frame work of rigid shell model (RSM) where short range interactions are effective upto the second neighbours and known as van der Waal's three body force shell model (VTSM).

2.1. Secular equations

For ZBS crystals, the cohesive energy for a particular lattice separation *(r)* has been expressed as

$$\Phi(r) = \Phi_{LR}(r) + \Phi_{SR}(r) \tag{1}$$

where the first term $\Phi_{LR}(r)$ represents the long-range Coulomb and three body interaction (TBI) energies expressed by

$$\Phi_{LR}(r) = -\sum_{\substack{ij \\ i\neq j\neq k}} \frac{Z_i Z_j e^2}{r_{ij}}\left\{1+\sum_k f(r_{ik})\right\} = -\frac{\alpha_M Z^2 e^2}{r}\left\{1+\frac{4}{Z}f(r)\right\} \tag{2}$$

where Z_i is the ionic charge parameter of i^{th} ion, r_{ij} separation between i^{th} and j^{th} ion, $f(r_{ik})$ is the three-body force parameter dependent on nearest-neighbour separation r_{ik} and is a measure of ion size difference Singh [19], α_M is Madelung constant (=1.63805 for ZBS).

The second term in equation (1) is short-range energy contributions from overlap repulsion and van der Waals interactions (VDWI) expressed as [30].

$$\Phi_{SR}(r) = Nb\sum_{i,j=1}^{2} exp\left[\frac{r_i + r_j - r_{ij}}{\rho}\right] - \sum_{ij}\frac{c_{ij}}{r_{ij}^6} - \sum_{ij}\frac{d_{ij}}{r_{ij}^8} \tag{3}$$

where *N* is the Avogadro's a number, b is the hardness parameters and the first term is the Hafemeister and Flygare (HF) potential Hafemeister and Flygare [31] and used by Singh and coworkers. The second term and third term represent the energy due to VDW for c_{ij} dipole-dipole (d - d) and d_{ij} dipole - quadrupole (d - q) interactions, respectively.

Using the crystal energy expression (1), the equations of motion of two cores and two shells can be written as;

$$\omega^2 \underline{M}\,\underline{U} = \left(\underline{R} + \underline{Z_m}\,\underline{C'}\,\underline{Z_m}\right)\underline{U} + \left(\underline{T} + \underline{Z_m}\underline{C'}\,\underline{Y_m}\right)\underline{W} \tag{4}$$

$$O = \left(\underline{T}^T + \underline{Y_m}\,\underline{C'}\,\underline{Z_m}\right)\underline{U} + \left(\underline{S} + \underline{K} + \underline{Y_m}\underline{C'}\,\underline{Y_m}\right)\underline{W} \tag{5}$$

Here $\underline{U}$ and $\underline{W}$ are vectors describing the ionic displacements and deformations, respectively. $\underline{Z_m}$ and $\underline{Y_m}$ are diagonal matrices of modified ionic charges and shell charges, respectively; $\underline{M}$ is the mass of the core; $\underline{T}$ and $\underline{R}$ are repulsive Coulombian matrices respectively; $\underline{C'}$ are long-range interaction matrices that include Coulombian and TBI; $\underline{S}$ and $\underline{K}$ are core-shell and shell-shell repulsive interaction matrices, respectively and $\underline{T}^T$ is the transpose of matrix $\underline{T}$. The elements of matrix $\underline{Z_m}$ consist of the parameter Z_m giving the modified ionic charge.

$$Z_m = \pm Z\sqrt{1+\left(\frac{8}{Z}\right)f(r_0)} \tag{6}$$

The elimination of $\underline{W}$ from eqns. (4) and (5) leads to the secular determinant;

$$\left|\underline{D}(\vec{q}) - \omega^2\underline{M}\,\underline{I}\right| = 0 \tag{7}$$

for the frequency determination. Here $\underline{D}$ (q) is the (6×6) dynamical matrix given by

$$\underline{D}(\vec{q}) = \left(\underline{R} + \underline{Z_m}\underline{C'}\,\underline{Z_m}\right) - \left(\underline{T} + \underline{Z_m}\underline{C'}\,\underline{Y_m}\right)\times\left(\underline{S} + \underline{K} + \underline{Y_m}\underline{C'}\underline{Y_m}\right)^{-1}\left(\underline{T}^T + \underline{Y_m}\,\underline{C'}\,\underline{Z_m}\right) \tag{8}$$

The numbers of adjustable parameters have been largely reduced by considering all the short-range interactions to act only through the shells.

2.2. Vibrational Properties of Zinc-Blende Structure

By solving the secular equation (4) along [q 0 0] direction and subjecting the short and long-range coupling coefficients to the long-wavelength limit $\vec{q} \to 0$, two distinct optical vibration frequencies are obtained as

$$(\mu\omega_L^2)_{q=0} = R_0' + \frac{(Z'e)^2}{vf_L}\cdot\frac{8\pi}{3}(Z_m^2 + 4Zr_0f'(r_0)) \quad (9)$$

$$(\mu\omega_T^2)_{q=0} = R_0' - \frac{(Z'e)^2}{vf_T}\cdot\frac{4\pi}{3}Z_m^2 \quad (10)$$

where the abbreviations stand for

$$R_0' = R_0 - e^2\left(\frac{d_1^2}{\alpha_1} + \frac{d_2^2}{\alpha_2}\right); R_0 = \frac{e^2}{v}\left[4\ \frac{A_{12}+2B_{12}}{3}\right];\ Z' = Z_m + d_1 - d_2 \quad (11)$$

$$f_L = 1 + \left(\frac{\alpha_1+\alpha_2}{v}\right)\cdot\frac{8\pi}{3}(Z_m^2 + 4Zr_0f'(r_0)) \quad (12)$$

$$f_T = 1 - \left(\frac{\alpha_1+\alpha_2}{v}\right)\cdot\frac{4\pi}{3} \quad (13)$$

and

$$\alpha = \alpha_1 + \alpha_2 \quad (14)$$

And $v = 3.08r_0^3$ for ZBS (volume of unit cell).

2.3. Debye Temperatures Variation

The specific heat at constant volume C_v at temperature T is expressed as

$$C_v = 3NK_B\frac{\int_0^{\upsilon_m}\left\{\left(\frac{h\upsilon}{K_BT}\right)^2 e^{h\upsilon/K_BT}\right\}G(\upsilon)d\upsilon \Big/ \left(e^{h\upsilon/K_BT}-1\right)^2}{\int_0^{\upsilon_m}G(\upsilon)d\upsilon} \quad (15)$$

where, υ_m is the maximum frequency, h is the Planck's constant and K_B is the Boltzmann's constant. The equation (15) can be written as a suitable form for a computational purpose as

$$C_v = 3NK_B\frac{\sum_\upsilon\{E(x)\}G(\upsilon)d\upsilon}{\sum_\upsilon G(\upsilon)d\upsilon} \quad (16)$$

where E(x) is the Einstein function, defined by

$$E(x) = x^2\frac{exp\,(x)}{\{exp(x)-1\}^2} \quad (17)$$

where $x = \left\{\left(\frac{h\upsilon}{K_BT}\right)^2 e^{\frac{h\upsilon}{K_BT}}\right\}$

Also,

$\sum_\upsilon G(\upsilon)d\upsilon$ = Total number of frequencies considered.

= 6000 for zinc- blende structure.

Hence, equation (16) can be written for zinc-blende structure type crystals, as

$$C_v = \frac{3NK_B}{6000}\sum_\upsilon E(x)G(\upsilon)d\upsilon \quad (18)$$

The contribution of each interval to the specific heat is obtained by multiplying an Einstein function corresponding to mid-point of each interval (say 0.1 THz) by its statistical weight. The statistical weight of the interval is obtained from the number of frequencies lying in that interval. The contributions of all such intervals, when summed up give, $\sum_\upsilon E(x)G(\upsilon)d\upsilon$. The Specific heat C_v is then calculated by expression (18).

2.4. Second and third order elastic constant

Proceeding with the use of three body crystal potential given by equation (1), (Sharma and Verma [21]) have derived the expressions for the second order elastic constants and used by (Singh and Singh [20]) for zinc-blende structure crystals. We are reporting them here as their corrected expressions.

The expressions for second order elastic constants (SOEC) are-

$$C_{11} = L\left[0.2477Z_m^2 + \frac{1}{3}(A_1 + 2B_1) + \frac{1}{2}(A_2 + B_2) + 5.8243Zaf'(r_0)\right] \quad (19)$$

$$C_{12} = L\left[-2.6458Z_m^2 + \frac{1}{3}(A_1 - 4B_1) + \frac{1}{4}(A_2 - 5B_2) + 5.8243Zaf'(r_0)\right] \quad (20)$$

$$C_{44} = L\left[-0.123Z_m^2 + \frac{1}{3}(A_1 + 2B_1) + \frac{1}{4}(A_2 + 3B_2) - \frac{1}{3}\nabla(-7.539122Z_m^2) + A_1 - B_1\right] \quad (21)$$

where $A_1 = A_{12}, B_1 = B_{12}, A_2 = A_{11} + A_{22}, B_2 = B_{11} + B_{22}$, $C_1 = \frac{A_{12}^2}{B_{12}}$ and $C_2 = \frac{A_2^2}{B_2}$

and the expressions for third order elastic constants (TOEC) are-

$$C_{111} = L\left[0.5184Z_m^2 + \frac{1}{9}(C_1 - 6B_1 - 3A_1) + \frac{1}{4}(C_2 - B_2 - 3A_2) - 2(B_1 + B_2) - 9.9326Zaf'(r_0) + 2.5220Za^2f''(r_0)\right] \quad (22)$$

$$C_{112} = L\left[0.3828Z_m^2 + \frac{1}{9}(C_1 + 3B_1 - 3A_1) + \frac{1}{8}(C_2 + 3B_2 - 3A_2) - 11.642Zaf'(r_0) + 2.5220Za^2f''(r_0)\right] \quad (23)$$

$$C_{113} = L\left[6.1585Z_m^2 + \frac{1}{9}(C_1 + 3B_1 - 3A_1) - 12.5060Zaf'(r_0) + 2.5220Za^2f''(r_0)\right] \quad (24)$$

$$C_{144} = L\left[6.1585Z_m^2 + \frac{1}{9}(C_1 + 3B_1 - 3A_1) - 4.1681Zaf'(r_0) + 0.8407Za^2f''(r_0) + \nabla\left\{-3.3507Z_m^2 - \frac{2}{9}C_1 + 13.5486Zaf'(r_0) - 1.681Za^2f''(r_0)\right\} + \nabla^2\left\{-1.5637Z_m^2 + \frac{2}{3}(A_1 - B_1) + \frac{1}{9}C_1 - 5.3138Zaf'(r_0) + 2.9350Za^2f''(r_0)\right\}\right] \quad (25)$$

$$C_{166} = L\left[-2.1392Z_m^2 + \frac{1}{9}(C_1 - 6B_1 - 3A_1) + \frac{1}{8}(C_2 - 5B_2 - 3A_2) - (B_1 + B_2) - 4.1681Zaf'(r_0) + 0.8407Za^2f''(r_0) + \nabla\left\{-8.3768Z_m^2 + \frac{2}{3}(A_1 - B_1) - \frac{2}{9}C_1 + 13.5486Zaf'(r_0) - 1.681Za^2f''(r_0)\right\} + \nabla^2\left\{2.3527Z_m^2 + \frac{1}{9}C_1 - 5.3138Zaf'(r_0) + 2.9350Za^2f''(r_0)\right\}\right] \quad (26)$$

$$C_{456} = L\left[4.897Z_m^2 + \frac{1}{9}(C_1 - 6B_1 - 3A_1) - B_2 + \nabla\left\{-5.0261Z_m^2 - \frac{1}{9}C_1\right\} + \nabla^2\left\{7.0580Z_m^2 + \frac{1}{3}C_1\right\} + \nabla^3\left\{-4.8008Z_m^2 + \frac{1}{3}(A_1 - B_1) - \frac{1}{9}C_1\right\}\right] \quad (27)$$

where Z_m is the modified ionic charge defined earlier with $L = e^2/4a^4$ and

$$\nabla = \left[\frac{-7.53912Z(Z+8f(r_0))+(A_1-B_1)}{-3.141Z(Z+8f(r_0))+(A_1+2B_1)+21.765Zaf'(r_0)}\right] \quad (28)$$

and Pressure derivatives of SOEC

$$\frac{dK'}{dP} = -(3\Omega)^{-1}[20.1788Z_m^2 + 3(A_1 + A_2) + 4(B_1 + B_2) + (C_1 + C_2) - 104.8433Zaf'(r_0) + 22.7008Za^2f''(r_0)] \quad (29)$$

$$\frac{dS'}{dP} = -(2\Omega)^{-1}\left[-11.5756Z_m^2 + 2(A_1 - 2B_1) + \frac{3A_2}{2} - \frac{7B_2}{2} + \frac{1}{4}\cdot C_2 + 37.5220Zaf'(r_0)\right] \quad (30)$$

$$\frac{dC_{44}'}{dP} = -(\Omega)^{-1}\left[\left\{0.4952Z_m^2 + \frac{1}{3}(A_1 - 4B_1 + C_1) + \frac{1}{2}\cdot A_2 - \frac{3}{2}\cdot B_2 + \frac{1}{4}\cdot C_2 + 4.9667Zaf'(r_0) + 2.522Za^2f''(r_0)\right\} + \nabla\left\{-17.5913Z_m^2 + A_1 - B_1 - \frac{2}{3}\cdot C_1 + 40.6461Zaf'(r_0) + 5.044Za^2f''(r_0)\right\} + \nabla^2\left\{3.1416Z_m^2 + \frac{2}{3}(A_1 - B_1) + \frac{1}{3}\cdot C_1 - 15.9412Zaf'(r_0) + 8.8052Za^2f''(r_0)\right\}\right] \quad (31)$$

where $K = \frac{C_{11}+2C_{12}}{3}$, $S = \frac{C_{11}-C_{22}}{2}$

and $\Omega = -5.0440Z_m^2 + (A_1 + A_2) - 2(B_1 + B_2) + 17.4730Zaf'(r_0)$

The values of *Ai*, *Bi* and *Ci* as defined by Sharma and Verma [21].

III. Computations

The model parameters (b, ρ and $f(r_0)$), have been determined by using the expressions (19-21) and the equilibrium condition $\left(\frac{d\Phi(r)}{dr}\right)_{r_0=a\frac{\sqrt{3}}{2}} = 0$, with the inclusion of the van der Waal's interactions (VDWI) [equation (3)]. The values of the input data K. Kunc. et al. [32] and P. H. Borcherds et al. [3] and model parameters have been shown in Table1. The values of A_i, B_i, C_i have been calculated from the knowledge of b, ρ; the values of various order of derivatives of $f(r_0)$ and van der Waal's coupling coefficients [21]. The values of VDW coefficients used by us in the present study have been determined using the Slatre-Kirkwood Variation (SKV) method [33], Lee [34] approach as suggested by Singh and Singh [20] and reported by Sharma and Verma [21]. Thus our model parameters are [b, ρ, $f(r_0)$, $r_0f'(r_0)$, A_{12}, A_{11}, A_{22}, B_{12}, B_{11}, B_{22}, d_1, d_2, Y_1 and Y_2]. The values of the van der Waal's coefficients (VDW) are shown in Table 2. Our model parameters of VTSM have been used to compute the phonon spectra of InP for the allowed 48 non-equivalent wave vectors in the first Brillouin zone. The frequencies along the symmetry directions have been plotted against the wave vector to obtain the phonon dispersion curves (PDCs). These curves have been compared with those measured by means of the coherent inelastic neutron scattering technique [3, 4] in Fig. 1 along with the BBFM calculations of Kunc. et al. [32]. Since the neutron scattering experiments provide us only very little data for the symmetry directions, we have also computed combined density of states (CDS) and the Debye temperatures variation for the complete description of the frequencies for the Brillouin zone.

The complete phonon spectra have been used to compute the combined density of states (CDS), $N(\upsilon_j+\upsilon_j')$ corresponding to the sum modes $(\upsilon_j+\upsilon_j')$ following procedure of Smart et al. [35]. A histogram between $N(\upsilon_j+\upsilon_j')$ and $(\upsilon_j+\upsilon_j')$ has been plotted and smoothed out as shown in Fig. 2. These curves show well defined peaks which correspond to two- phonon Raman scattering. These CDS peaks have been compared with the assignments calculated and shown in Table 3. The Debye temperatures variation for InP measured from by U. Piesbergen [17] and those calculated by us using VTSM has been compared in Fig.3. The calculated values of TOEC using equations (22-27) have been compared with calculated values of Sadao Adachi [36] and shown in Table 4. The pressure derivatives of SOEC have also been calculated and compared with those measured by D. Wolf Gerlich [37] in Table 5.

IV. Results and discussion

4.1 Phonon Dispersion Curves

From figure1, our phonon dispersion curves for InP agree well with measured data reported by Borcherds et al. [3]. It is evident from PDCs that our predictions using present model (VTSM) are better than those by using BBFM [32]. Our model has successfully explained the dispersion of phonons along the three symmetry directions. From fig.1 and Table 6, it is clear that: there are deviations of 2.11% along LO(X), 4.43% along TO(X), 8.10% along LA(X), 9.76% along TA(X), 0.29% along LA(L) and 2.95% along TA(L) from experimental results. From BBFM, deviations are 9.76% along TA(X), 8.10% along LA(L) and 21.21% along TA(L) while from VTSM 0.00% along TA(X), 1.00% along LA(L) and 0.00% along TA(L). From table 6 it is clear that VTSM has very small deviation from experimental data. Our model VTSM has 21.21% improvement over BBFM due to inclusion of three body interactions (TBI) and VDWI coefficients. Therefore, our VTSM model has better agreement with experimental data over BBFM [32].

4.2. Combined Density of States

The present model is capable to predict the two phonon Raman spectra [18]. The results of these investigations for combined density states (CDS) peaks have been presented in Fig. 2. The theoretical peaks are in good agreement with observed Raman peaks for InP. The assignments made by the critical point analysis have been shown in Table 3. The interpretation of Raman spectra achieved from both CDS approach and critical point analysis is quite satisfactory. This explains that there is an excellent agreement between experimental data and our theoretical results. There is no any experimental data available for InP of two phonon IR spectra. So we could not report comparison of combined density states (CDS) peaks for IR spectra.

4.3. Third Order Elastic Constants (TOEC) and Pressure Derivatives of Second Order Elastic Constants (SOEC)

Our calculations on TOEC of InP have been compared with the theoretical results of Sadao Adachi [36]. Further, pressure derivatives of SOEC for InP have also been compared with the measured data of D. Gerlich, and M. Wolf, [37] as shown in Table 5. The results are in good agreement.

4.4. Debye Temperatures variation

From Fig. 3, our study shows a better agreement with the measured data of U. Piesbergen [17] and the theoretical results of BBFM [32]. We can say that our present model gives a better interpretation of the Debye temperatures variation for InP.

V. Conclusion

The inclusion of van der Waal's interactions (VDWI) with TBI have influenced both the optical branches and the acoustic branches. Another striking feature of present model is noteworthy from the excellent reproduction of almost all branches of PDCs, Hence the prediction of phonon dispersion curves (PDC) for InP using VTSM may be considered more satisfactory than from other model [32]. The basic aim of the study of two phonon Raman spectra is to correlate the neutron scattering and optical measured data of InP. In this paper, we have systematically reported phonon dispersion curves, combined density of states, Debye temperatures variation and a part of harmonic and anharmonic properties of InP. On the basis of overall discussion, it is concluded that our van der Waal's three body force shell model (VTSM) is adequately capable of describing the crystal dynamics of indium phosphide. This model may also be applied equally well to study the crystal dynamics of other compounds of this group (InAs and InSb). Our work gets strong support from paper of Mishra and Upadhyaya [27] and Dubey et. al. [28, 29].

Acknowledgements

The authors are thankful to Computer Center, BHU, Varanasi, India for providing computational assistance. One of us Jay Prakash Dubey is gratitude to Dr. Devendra Pathak, vice chancellor, Dr. K. N. Modi University Newai, Rajasthan, India for encouragement and providing necessary facilities during research work. I am also thankful to Dr. Pramod Kumar Pandey, Professor, Department of Physics, Pt. S. N. S. Govt. P. G. College, Shahdol (M. P.), India for their guidance.

References

[1]. Henion B., Moussa F., Pepy G. and Kunc K., Phys. Lett. 36 A, 376 (1971)
[2]. Yarnell J. L., Warren J. L., Wenzel R. G. and Dean P. J., Newtron inslantic scattering I (International atomic energy Agency, Vienna, 301 (1968)
[3]. Borcherds P. H., Alfrey G., Sauderson D. H. and Wood A. D. B., Phys. C 8, 2022 (1975)
[4]. Ram R. K., Kushwaha M. S. and Shukla A., Phys. Stat. Solidi B 154, 553 (1989)
[5]. Vegeletos N., Wehe D. and King J. S., Journal Chem. Phys. 60, 3813 (1974)
[6]. Vetelino J. F. and Mitra S. S., Phys. Rev. 178, 1349 (1959)
[7]. Vetelino J. F., Mitra S. S., Brafman O. and Damen T. C., Solid State Commun. 7, 1809 (1969)
[8]. Vetelino J. F. , Mitra S. S., Namjoshi Brafman, Joshi K.V., Phys. Rev., B2, 967 (1970) Rev., 112, 90 (1958)
[9]. Cochran W. , Proc. W., R. Soc. London A253, 260 (1959); Adv. Phys.9, 387 (1960)
[10]. Banerjee R. and Varshni Y. P., Canad. J. Phys., 47, 451 (1960) ; J. Phys. Soc. JPn., 30, 1015 (1971)
[11]. Price D. L., Rowe J. M. and Nicknow R. M., Phys. Rev. B3, 1268 (1971)
[12]. Talwar D. N. and Agrawal B. K., Phys. Rev. B8, 693 (1973); Solid State Commun., 11, 1691 (1972)
[13]. Feldkamp L. A., Steinman D. K., Vegelotos N., King J. S. and Venkataraman G. J., J. Phys. Chem. Solid, 32, 1573 (1971)
[14]. Varshni Y. P., Canad. J. Phys., 47, 451 (1960)
[15]. Weber W., Phys. Rev. Lett., 33, 371 (1974)
[16]. Gerlich D. and Wolf M.; High Pressure Sci. technol., 1, 506 (1980)
[17]. Piesbergen U., Semiconductors and Semimetals 2, 49 (1966).
[18]. Alfray G. F. and Borcherds P. H., J. Phys. C 5, 1275 (1972)
[19]. Singh, R. K. Physics Reports (Netherlands), 85, 259 (1982)
[20]. Singh, R. K., Singh, S., Phys. Status Solidi (b) 140, 407 (1987)
[21]. Sharma, U. C. and Verma, M. P. Phys. Status Solidi (b) 102, 487 (1980)
[22]. Garg V. K., Puri D. S., Verma M. P. Phys. Status Solidi (b) 87, 401 (1978)
[23]. Upadhyaya, K. S., Pandey, A, Srivastava, D. M. Chinese J. Phys. 44, 127 (2006)
[24]. Upadhyaya, K. S., Upadhyay, G. K., Yadav, M., Singh, A. K., J. Phys. Soc. Japan, 70, 723 (2001)
[25]. Tiwari, S. K., Pandey, L. K., Shukla, L. J., Upadhyaya, K. S., Phyica Scr., 80, 065603 (2009)
[26]. Srivastava, U. C., Upadhyaya, K. S., Physcial Rev. and Res. Int., 1, 16 (2011)
[27]. Mishra, K. K., Upadhyaya, K. S., Int., Jour. Sci. Engg. Res., 3, 1388 (2012)
[28]. Dubey J. P., Tiwari R. K., Upadhyaya K. S. and Pandey P. K., Turk. J. Phys. 39, 242 (2015)
[29]. Dubey J. P., Tiwari R. K., Upadhyaya K. S. and Pandey P. K., Jour. of Appl. Phys. (IOSR-JAP) 7, 67 (2015)
[30]. Singh R. K. and Khare P. J. Phys. Soc. Japan 51, 141 (1982)
[31]. Hafemeister D. W. and Flygare W. H. J. Chem. Phys. 43, 795 (1965)
[32]. Kunc K., Balkanski M. and Nusimovici M. A. Phys. Status Solidi (b) 72, 229 (1975)
[33]. Slater J. C. and Kirkwood J. G. Phys. Rev. 37, 682 (1931)
[34]. Lee B. H. J. Appl. Phys. 41, 2988 (1970)
[35]. Smart C., Wilkinson G. R. and Karo A. M., Lattice Dynamics, edited by Wallis R. F. (1965)
[36]. Sadao Adachi; Semiconductor Wiley series in materials for Electronic and opto electronic Application. Department of Electric Engineering Gunma University Japan (1956)
[37]. Gerlich, D. and Wolf, M. High pressure Sci. Technol. 1, 506 (1980)

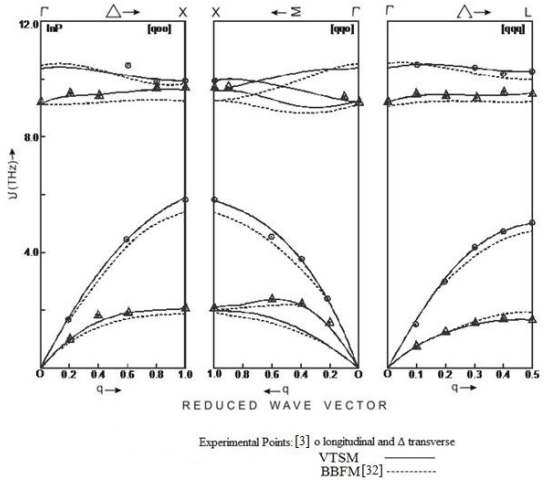

Figure 1: Phonon dispersion curves for InP

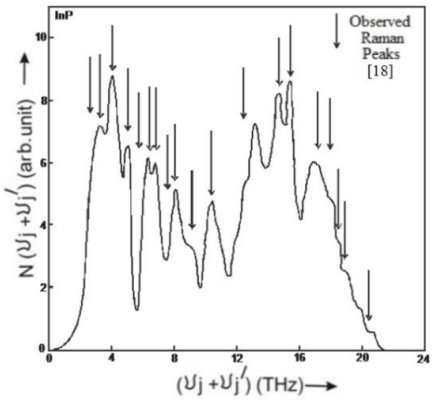

Figure 2: Combined density of states curve for InP

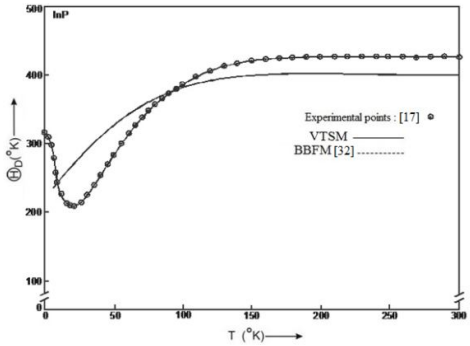

Figure 3: Debye characteristics temperatures Θ_D (°K) as a function of temperature T for InP

Table 1. Input data and model parameters for InP [C_{ij} and B (in 10^{11} dyne/cm^2), υ (in THz), r_0 (in 10^{-8} cm),α_i (in 10^{-24} cm^3), b (in 10^{-12} erg), ρ (in 10^{-8} cm)]

Input Data		Model Parameters	
Properties	Values	Parameters	Values
C_{11}	10.22[a]	b	1.05
C_{12}	5.76[a]	ρ	0.341
C_{44}	4.60[a]	$f(r_0)$	–0.28
B	7.25[b]	$r_0 f'(r_0)$	0.111
r_0	2.54[a]	A_{12}	3.068
$\upsilon_{LO}(\Gamma)$	10.46*	B_{12}	–16.209
$\upsilon_{TO}(\Gamma)$	9.20[b]	A_{11}	41.598
$\upsilon_{LO}(L)$	10.20[b]	B_{11}	–5.3672
$\upsilon_{TO}(L)$	9.5[b]	A_{22}	–5.722
$\upsilon_{LA}(L)$	5.0[b]	B_{22}	–3.656
$\upsilon_{TA}(L)$	1.65[b]	d_1	0.1237
α_1	0.221[a]	d_2	3.5245
α_2	6.8449[a]	Y_1	–1.1615
ε_0	12.40[a]	Y_2	–1.2626

*Extrapolated values from [3].
[a]-(K. kunc. et al. [32]); [b]- (P. H. Borcherds et al. [3])

Table 2. van der Waal's Interaction Coefficients for InP (C_{ij} and C in units of 10^{-60} erg cm^6 and d_{ij} and D in units of 10^{-76} erg cm^8)

Parameters	Numerical Values
C_{+-}	494
C_{++}	372
C_{--}	721
d_{+-}	387
d_{++}	189
d_{--}	704
C	2569
D	1690

Table 3. Assignments for the observed peak positions in Combined Density of States in terms of selected phonon frequencies at Γ, X and L critical points for InP

CDS Peaks (cm^{-1})	Raman Active		
	Observed Raman Peaks (cm^{-1}) [18]	Present Study	
		Values (cm^{-1})	Assignments
.....	85	87	LA-TA (Δ)
107	107	110 110	2TA(L) LA-TA (L)
133	135	136	2TA (X)
163	163	170	TO-LA(Δ)
.....	189	190	LO-LA(Δ)
213	214	213	LA-TA(Δ)
227	228	220	LA+TA (L)
.....	251	257	LO-LA (L)
268	269	263	LA+TA (X)
305	304	300	2LA(Δ)
343	346	.....	…..
410	412	.....	…..
492	490	490	LO+LA(Δ)
513	510	517	LO+LA(X)
573	573	.....	.....
593	596	.....	……
.....	620	614	2TO(Γ)
630	626	634	2LO(L)
683	684	680	2LO(Δ)

Table 4. Third Order Elastic Constants (in the unit of 10^{11}dyne/cm^2) for InP

Property	Present Study	Experimental Results [36]
C_{111}	–9.216	–8.60
C_{112}	–2.346	–1.85
C_{123}	–5.927	–5.1
C_{144}	–7.927	–6.5
C_{166}	+2.16	+1.6
C_{456}	0.1325	–0.042

Table 5. Values of pressure derivatives of SOEC (in dimensionless) for InP

Properties	Values		
	Present Study	Experimental [16]	Other [37]
dK'/dP	5.2	4.88	4.50
dS'/dP	–0.233	-0.29	-0.89
dC'_{44}/dP	0.80	0.26	0.79

Table 6. Comparison of frequencies from various sources (X and L points) for InP

Points	Branches	Expt. [3] (THz)	BBFM [32]			VTSM (Present Study)			% Improvement Over BBFM (a ~ b)
			Value (THz)	(±) Deviation	% (a)	Value	(±) Deviation	% (b)	
X (100)	LO	9.95	9.74	0.21	2.11	10.0	0.05	0.50	1.61
	TO	9.70	9.22	0.43	4.43	9.65	0.05	0.86	7.24
	LA	5.8	5.33	0.47	8.10	5.85	0.05	0.86	7.24
	TA	2.05	1.85	0.20	9.76	2.05	0.00	0.00	9.76
L (.5.5.5)	LO	10.2	9.99	0.03	0.29	10.15	0.05	0.49	0.20
	TO	9.5	9.22	0.28	2.95	9.50	0.00	0.00	2.95
	LA	5.0	4.72	0.18	3.60	4.95	0.05	1.00	2.6
	TA	1.65	2.00	0.35	21.21	1.65	0.00	0.00	21.21